Inverter operating characteristics optimization for DC traction power supply systems

Zhang, Gang; Tian, Zhongbei; Tricoli, Pietro; Hillmansen, Stuart; Wang, Yong; Liu, Zhigang

DOI:
10.1109/TVT.2019.2899165

Inverter Operating Characteristics Optimization for DC Traction Power Supply Systems

Gang Zhang, Zhongbei Tian, Pietro Tricoli, Stuart Hillmansen, Yong Wang and Zhigang Liu

***Abstract*—Compared with energy storage equipment based on supercapacitors, flywheels or lithium batteries, inverters have obvious advantages in installation space, cost, reliability and service lifetime. For this reason, regenerative inverters are increasingly installed in the substations of urban rail transit systems. They have controllable operating characteristics, but their impact on the energy saving and railway operation cost has not been fully studied. In this paper, based on the typical application scheme of regenerative inverters, the operating characteristics of the inverter including power limitation, start working voltage, virtual internal resistance are introduced at first. A simplified power system model containing regenerative inverters and trains has been built. The impact of operating characteristics on the amount of regenerative braking energy and its distribution is analyzed. The inverter operating characteristics are optimized by a cost function considering total energy consumption, brake shoes wear and inverter expense. A case study based on a multi-train scenario is presented to validate the cost-saving performance. The work is expected to provide some guides for the design and optimization of the traction power supply system with inverting substations.**

***Index Terms*—energy consumption, optimization, traction power supply systems, inverter, railway simulation, cost function**

I. INTRODUCTION

The reduction of energy consumption has become essential due to climate changes taking place as a result of enormous green gas emission. Urban rail transit system is becoming an increasingly popular choice to satisfy transportation demands all over the world because of its relatively low ratio between energy consumption and transport capacity [1].

All modern trains have regenerative braking capability, converting the kinetic energy into electricity. The regenerative braking is widely used because of two major reasons. One reason is that the regenerative braking is eco-friendly. In contrast to friction braking, regenerative braking does not generate wear and tear, dust, smell, heat and sound. The other reason, the most important one, is attributed to its huge potential in energy saving. The recovered energy will firstly be used to supply the auxiliary load on the train itself, and the surplus energy will then be provided to the other accelerating trains on the same DC network. Theoretically, the regenerative braking power could be completely reused if there are always accelerating trains nearby requiring higher power at the same time. However, this is impossible in practice. The DC network is not always receptive. To avoid the DC overvoltage due to too much regenerative braking energy, the surplus energy is usually dissipated by the on-board resistors, causing energy waste and tunnel temperature rise [2].

In order to maximize the utilization of regenerative braking energy and reduce the energy consumption, the thyristor-based inverters were introduced to feed the recovered braking energy back to medium voltage distribution grid (MVDG) for reuse [3-5]. However, this kind of inverter is not widely applied in the DC railway due to its poor power quality and bad cost-performance. The installation of energy storage devices (such as super-capacitor, lithium battery or flywheel) at substations or tracksides could be a good alternative to absorb the surplus regenerated energy and regulate DC voltage [6-12]. However, compared with inverters, some drawbacks of energy storage system are bigger installation space, higher cost, shorter service life and more safety constraints [13].

In recent years, with the technology development of power semiconductor IGBT and converter control, the cost-effective IGBT inverters have been increasingly employed in DC traction power supply system [14-19]. Traction substations with inverters are called inverting substations or reversible substations. Up to now, the regenerative inverters have been used in more than 20 metro lines in China. The energy saving of inverters installed in Beijing Metro line 10 of China achieves as high as 11.15% of daily use [20]. Regarding low-order current harmonic generated by the diode rectifier, the inverter is proposed to work as an active power filter in some literature [21-24] , so as to improve the utilization ratio of the inverter. To solve the low power factor problem in the light load period, which is caused by the large amount of stray capacitance of the medium voltage ring cables, the traditional schemes based on Static Var Generator (SVG) are usually adopted [25, 26]. In fact, the SVG can be reduced or cancelled when regenerative inverters are installed in the substations, which have been verified in Zhengzhou metro line 2 and Chengdu metro line 7 in China. In this case, the payback period of the regenerative inverters will be shortened significantly.

This research was supported by the Fundamental Research Funds for the Central Universities (2018JBZ004). (*corresponding author: Zhongbei Tian)*

G. Zhang is with School of Electrical Engineering, Beijing Jiaotong University, Beijing 100044, China (e-mail: gzhang@bjut.edu.cn).

Z. Tian, P. Tricoli and S. Hillmansen are with Department of Electronic, Electrical and Systems Engineering, University of Birmingham, Birmingham B152TT, UK (e-mail: z.tian@bham.ac.uk, p.tricoli@bham.ac.uk, s.hillmansen@bham.ac.uk).

Y. Wang is with Institute of standards and metrology, China academy of railway sciences group co., LTD, Beijing 100081, China (e-mail:15210261167@163.com.cn).

Z. Liu is with Beijing Electrical Engineering Technology Research Center, Beijing 100044, China (e-mail: zhgliu@bjtu.edu.cn).

Although inverters have been used in traction power supply system (TPSS) for several years, few literature discusses the optimization of the operating characteristics for regenerative inverters. The most commonly used operating characteristics of the inverter used in railway substation is constant voltage control [27-29]. It is easy to implement and beneficial for the stabilization of DC network voltage. However, the serious unbalanced distribution of regenerative braking energy between substations will happen, which is not good for the reuse of the energy in the medium voltage grid. Two possible inverter control schemes: the constant advance angle control and the constant voltage control were illustrated in [3, 4], but the impact of operating characteristics on the energy saving and energy distribution were not studied. In addition, the capacity configuration of inverters in TPSS usually depends on system simulation [27, 28], but in most existing simulation systems, an inverter is simply modeled as an ideal voltage source or a voltage source with internal resistance. The power limitation of the inverter is not considered in the inverter model. It will bring obvious error in the simulation results, which cannot be neglected.

This paper proposes a modeling method considering the different operating characteristics of inverters including power limitation, start working voltage, virtual internal resistance. An approach to optimize operating characteristics of inverters for cost saving is illustrated. This paper is organized as follows. The section II introduces application scheme and operating characteristics of inverters. In section III, impact of inverter operating characteristics on the energy-saving and regenerative braking energy distribution is analyzed based on a simplified system model, then an optimization strategy is proposed. In section IV, optimization of inverter operating characteristics considering multi-trains scenario is carried out by a case study. The conclusions are presented in section V.

II. Operating Characteristics Modeling

A. Application scheme of inverters

The typical application scheme of inverters in the TPSS is shown in Fig. 1. It can be seen that the IGBT based inverters are added to each traction substation in parallel with the conventional diode rectifier (DR). C_{eq} denotes the equivalent capacitance of the medium voltage cable. T_1 and T_2 denote the step-down transformer in the main substation (MS). bus_1 and bus_2 represent two medium voltage grids, which will be interconnected through breaker Q only when T1 or T2 happens to be fault. All traction substations are alternately connected to bus_1 or bus_2. With inverters, the surplus regenerative braking energy of the trains can be converted back to medium voltage grid, supplying the AC load. Thus, the electricity energy provided by Power Grid Corporation (PGC) can be obviously reduced.

Besides recovery of regenerative braking energy, the inverters can also generate a certain amount of reactive power to improve the power factor of the medium voltage grid, replace the special reactive power compensation equipment such as SVG. As an auxiliary function, it will increase the utilization rate of inverter, shorten investment payback period. But this is not the focus of this paper.

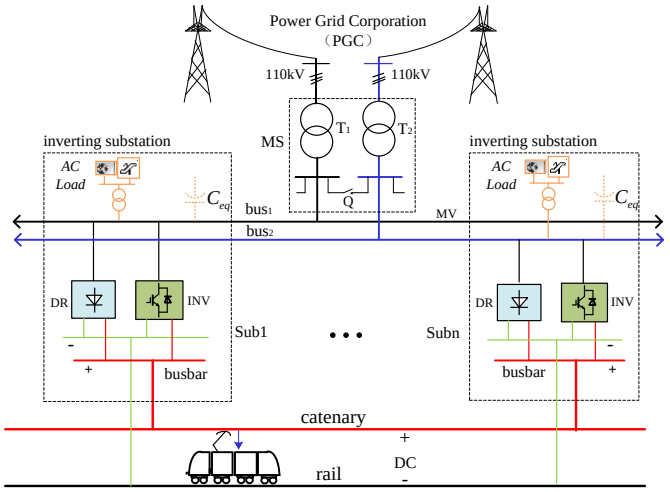

Fig. 1.Typical application scheme of inverter in the TPSS

B. Operating characteristics of inverters

The main circuit of two-level voltage source inverter is shown in Fig. 2. T is the transformer, L is the filter inductance, C is the filter capacitance of DC-Link, $Q_1 \sim Q_6$ are IGBTs. U_{dc} denotes the DC voltage, I_{dc} denotes the DC current, e_{abc} is the transformer secondary voltage, and e_{grid} is the AC grid voltage.

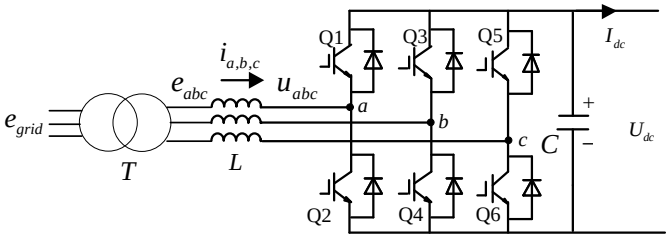

Fig. 2. Main circuit of the inverter used in a substation

The typical operating characteristic curve of the inverter is shown in Fig. 3. U_{st} is the start working voltage of the inverter, r is the virtual internal resistance, P_{max} is the power limitation (that is also the inverter power capacity), U_M is the maximum DC voltage , and U_k is the no-load voltage of diode rectifier.

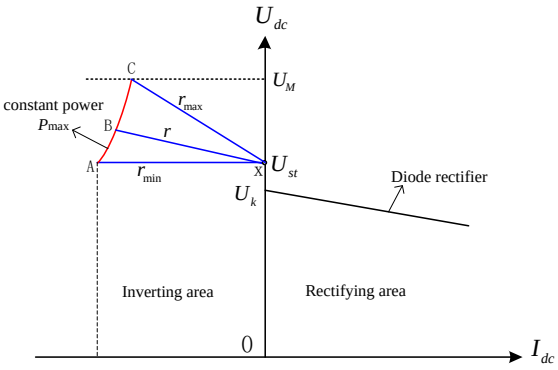

Fig. 3. Typical operating characteristic curve of an inverter

1) Linear inverting region

When inverter DC voltage is higher than U_{st}, the inverter will operate in the linear inverting region. The VI characteristic curve can be expressed as:

$$U_{\mathrm{dc}} = U_{\mathrm{st}} - r \times I_{dc} \tag{1}$$

where

$$\begin{cases} U_{\mathrm{st}} \le U_{\mathrm{dc}} \le U_M \\ r_{min} \le \mathrm{r} \le r_{max} \\ U_{\mathrm{dc}} \times I_{dc} \le P_{max} \\ I_{dc} \le 0 \end{cases} \tag{2}$$

The DC voltage keeps constant in the line XA, where the virtual internal resistance has a minimum value $r_{min} = 0$. The maximum virtual internal resistance of the inverter in the line XC can be written as:

$$r_{max} = \frac{\Delta U}{\Delta I} = \frac{U_M - U_{st}}{P_{max}/U_M} \tag{3}$$

2) Constant power region

When transferred power reaches the maximum value, the inverter operates on the constant power curve (ABC), which can be expressed as:

$$P_{dc} = U_{dc} \times I_{dc} = P_{max} \tag{4}$$

The DC side equivalent circuit of inverter is shown in Fig. 4, P_{ac} denotes the active power of inverter at AC side, i_{d} denotes the d-axis current, e_d denotes the d-axis voltage of the grid. Neglecting the conversion loss, the DC power P_{dc} of the inverter is equal to AC power P_{ac}, which is mainly determined by i_{d} when e_d keeps constant. In this case, the control of i_{d} becomes essential. It is worth noting that the DC voltage of inverter is controllable, but the DC current cannot be controlled directly. I_{dc} is mainly determined by load (trains). The constant power curve in Fig. 3 (curve ABC) is realized by limiting the d-axis current i_{d}.

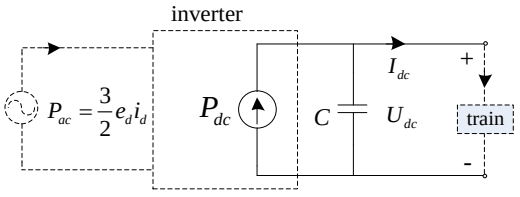

Fig. 4. DC side equivalent circuit of the inverter

In addition, in order to avoid the circulating current between the inverter and diode rectifier, the start working voltage of the inverter should be higher than the no-load voltage of diode rectifier, that is $U_{\mathrm{st}} > U_k$. To obtain the above operating characteristics in Fig. 3, the control scheme shown in Fig. 5 is adopted, which includes a DC voltage loop, a dq current loop and a droop control unit [20]. U_{dc}^* is the DC voltage reference which is calculated by droop control unit. i_d^* is the active current reference that calculated by DC voltage loop. LIM2 is a limitation unit for active current reference, which also limits the inverting power transferred by the inverter.

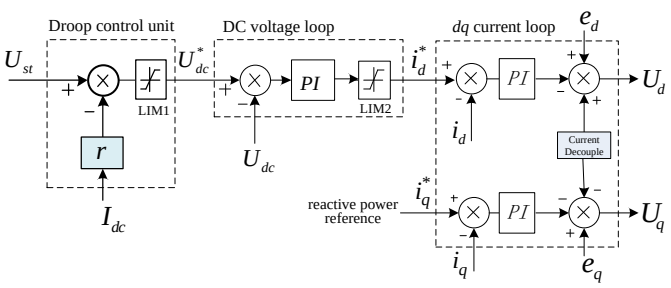

Fig. 5. Control scheme of inverter

C. Characteristics of a train

With respect to the traditional modeling method, a train is usually regarded as a time-dependent power source load. However, for improving the accuracy of train model, pantograph voltage should be taken into consideration. The interaction between trains and the traction network is analyzed in reference [30]. In case of a high voltage hazard, the regenerative braking will be cancelled to avoid the happen of the over-voltage protect. Fig. 6 shows the maximum allowable regenerative braking power against pantograph voltage of a train when on-board braking rheostats have not been installed. The train regenerative braking ability can be completely used when pantograph voltage is lower than U_1. Whereas if pantograph voltage is higher than U_1, the regenerative braking ability will face a linear decline, till becomes zero when voltage reaches U_2. To maintain a constant deceleration, the friction braking has to join in, resulting in serious braking energy lost.

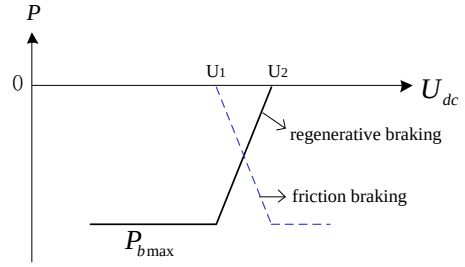

Fig. 6. Maximum allowable regenerative braking power against pantograph voltage

The maximum allowable regenerative braking power can be written as :

$$P_{limit} = \frac{U_2 - U_{tr}}{U_2 - U_1} \cdot P_{bmax}, \quad U_1 < U_{tr} < U_2 \tag{5}$$

where U_{tr} is the pantograph voltage of the train, P_{bmax} is maximum regenerative braking power without regeneration cancellation.

III. Impact Analysis and Optimization Strategy

A. Mathematical analysis

For a DC railway line with n traction substations, each substation is equipped with one inverter. The simplified system model is shown in Fig. 7, $U_{\mathrm{sub}i}$ and $I_{\mathrm{sub}i}$ represent the voltage and current of the i^{th} substation, respectively. R_{ij} represents the

equivalent resistance between the i^{th} and j^{th} substation, and P_{btr} represents the braking power of the train. S_w denotes the selection switch in the substation model to make a choice between voltage source and power source. The arrows in the figure represent the reference direction of current.

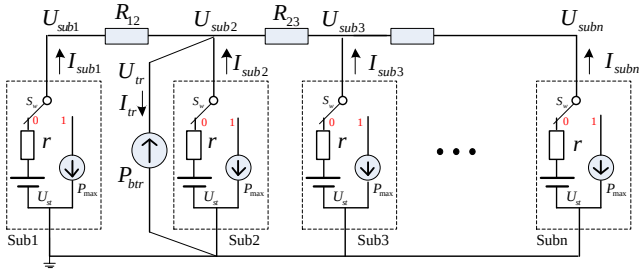

Fig. 7. System model with one braking train

For the convenience of analysis, it is assumed that the station distance is equal, that is $R_{12} = R_{23} = R_{ij} = R$, and no inverter reaches maximum power, that is $S_w = 0$. According to Thevenin's theorem, the linear two-terminal circuit can be replaced by an equivalent circuit comprised of an equivalent voltage source U_{eq} in series with an equivalent resistor r_{eq}. The network in Fig. 7 can be simplified as shown in Fig. 8.

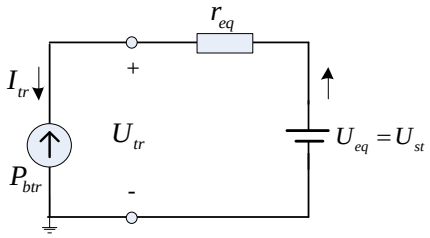

Fig. 8. Equivalent circuit based on Thevenin's theorem

Considering the limited transmission distance of braking energy due to the catenary and track resistance, only four substations (sub1-sub4) and a train are taken as a typical case for further mathematical analysis.

Given the train is braking at sub2, the system equivalent resistor r_{eq} in Fig. 8 can be expressed in (6).

$$r_{eq} = \frac{r^4 + 4Rr^3 + 4R^2r^2 + R^3r}{4r^3 + 10Rr^2 + 6R^2r + R^3} \tag{6}$$

The expression of the train voltage can be obtained:

$$U_{\mathrm{tr}} = \frac{U_{\mathrm{st}} + \sqrt{U_{\mathrm{st}}^2 + 4P_{\mathrm{btr}}r_{\mathrm{eq}}}}{2} \tag{7}$$

According to (6) and (7), the relation curves of network equivalent resistor r_{eq} and train voltage U_{tr} against virtual internal resistance r can be obtained as shown in Fig. 9, where the interstation distance is assumed to be 2km and interstation resistance R= 0.02Ω. It can be seen from Fig. 9(a) that r_{eq} has an obvious increasing trend with r. It can be observed from Fig. 9(b) that in case of the same braking power P_{btr}=3MW, the train voltage increases with r. In addition, the train voltage curve has an upward shift if the starting working voltage U_{st} increases from 850V to 900V. In fact, when the train voltage exceeds a certain value (U_1 in Fig. 6), the regenerative braking power will have to be reduced to avoid the over-voltage protect. Therefore, to ensure the regenerative braking ability of the train, U_{st} and r should be as small as possible.

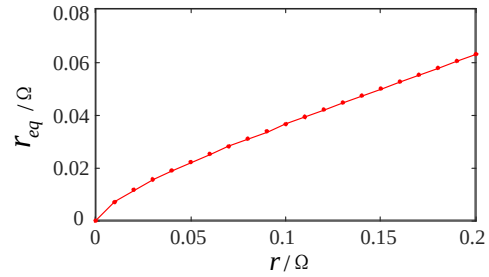

(a)

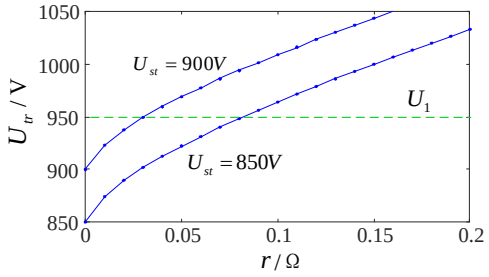

(b)

Fig. 9. Relation curves: (a) r_{eq} against r. (b) U_{tr} against r

To analyze the distribution of train regenerative braking current among sub1-sub4, taking the current of sub2 as the base value, then current of the four substations can be expressed as:

$$\begin{cases} I_1^* = \dfrac{I_{\mathrm{sub1}}}{I_{\mathrm{sub2}}} = \dfrac{k}{k+1} \\ I_2^* = \dfrac{I_{\mathrm{sub2}}}{I_{\mathrm{sub2}}} = 1 \\ I_3^* = \dfrac{I_{\mathrm{sub3}}}{I_{\mathrm{sub2}}} = \dfrac{k^2+k}{k^2+3k+1} \\ I_4^* = \dfrac{I_{\mathrm{sub4}}}{I_{\mathrm{sub2}}} = \dfrac{k^2}{k^2+3k+1} \end{cases} \tag{8}$$

where $k = r/R$, r represents the virtual internal resistance of substation, R represents the interstation resistance.

According to Fig. 1, sub1 and sub3 are connected to the bus1 of the medium voltage grid, sub2 and sub4 are connected to bus2 of the medium voltage grid. Therefore, the current balance coefficient B_r can be defined as:

$$B_r = \frac{I_1^* + I_3^*}{I_2^* + I_4^*} = \frac{2k^3 + 5k^2 + 2k}{2k^3 + 5k^2 + 4k + 1} \tag{9}$$

Fig. 10 shows the current distribution trend against k. It can be seen that with the increase of k, the difference among I_1^*, I_2^*, I_3^* and I_4^* is reduced, meanwhile B_r is approaching 1. This means that a greater k leads to a better current distribution balance between substations, also a better power balance between two power buses of medium voltage grid.

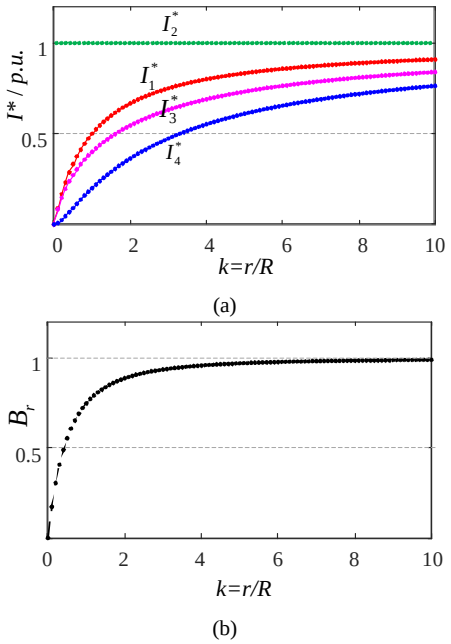

Fig. 10. Current distribution trend: (a) current against k. (b) B_r against k

Corresponding results can be obtained when the train brakes at other substations. It should be noted that the above analysis is based on the premise that no inverter reaches its power limitation, otherwise the inverter has to be equivalent to a power source, and the whole traction power supply network will become a nonlinear network. In this case, the exact analytical expression of current and voltage at each node cannot be easily given.

B. *Simulated analysis*

To assess the impact of the inverter operating characteristics, a static simulation model including four substations (sub1-sub4) and a train is built. The train is exactly located at the sub2 with regenerative braking power of 3MW, and U_1 =950V, U_2 =1000V. The interstation conductor line resistance is R=0.04. The inverter virtual internal resistance r varies from 0 to 0.18 with a step length Δr =0.02. The inverter power limitation P_{max} is 1MW or 2MW, and the start working voltage U_{st} is 850V or 900V. Fig. 11 shows the voltage and current of train and each substation under different conditions. I_{tr} and I_{sub} represent the current of train and substation, respectively. U_{tr} and U_{sub} represent the voltage of train and substation, respectively. In each subfigure, the VI results with various r (from 0 to 0.18) are labeled by {1} to {10}.

Fig. 11(a) shows the VI results with various r when P_{max}=2MW and U_{st}=850V. It can be found that when r=0, the current of sub2 is always the largest, the current of sub1 and sub3 are the same, and the current of sub4 is zero. The train voltage is 860V, a little higher than start working voltage U_{st} of inverter. The train voltage is the same with the sub2 voltage, because the train brakes at sub2. The inverting power of sub2 reaches its maximum allowable value 2MW. It means that sub2 is working in the constant power region (ABC) as shown in Fig. 3. However, with the increase in r, the current of sub2 decreases, and the current of other substations increase. The current difference between substations is reduced. At the same time, the voltage of train and substations increases with *r*. When $r > 0.10$, the train voltage exceeds 950V, and the regenerative braking ability is weakened.

Fig. 11(b) shows the VI results with various r when P_{max}=1MW and U_{st}=850V. When r=0, compared with Fig. 11(a), the current difference between substations is smaller due to the reduction of inverter capacity (from 2MW to 1MW). However, the train voltage becomes as high as 872V. The sub2 will keep working on the constant power curve until $r > 0.06$. The voltage of train and substations has the similar changing trend with r to the results when P_{max}=2MW. Therefore, the decrease in power capacity improves the average distribution of inverting power and increase the train voltage.

Fig. 11(c) shows the VI results with various r when P_{max}=1MW and U_{st}=900V. It can be found that the current difference between substations does not change a lot compared to U_{st}=850V. However, the voltage of train and substation have a nearly 50V increment with the same *r*. Therefore, the train voltage can exceed 950V easily. In order to maximize the regenerative braking ability of the train, U_{st} should be as low as possible.

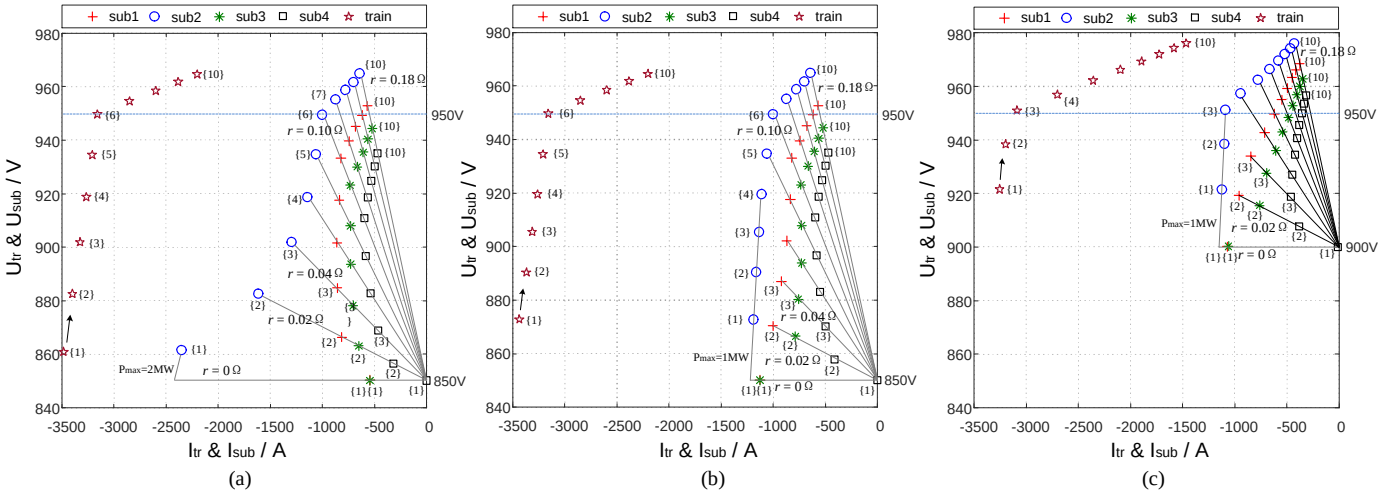

Fig. 11. Voltage and current of train and each substation in different conditions: (a) when P_{max}=2MW,U_{st}=850V. (b) when P_{max}=1MW,U_{st}=850V. (c) when P_{max}=1MW,U_{st}=900V .

C. Optimization strategy

In this paper, the aim of optimizing inverter operating characteristics is to achieve better energy savings and less brake shoes wear with less inverter investment. Therefore, the following objectives are considered [31-32].

1) Cost of total energy consumption, C_{elec}

In many countries, the PGCs only allows users to get electricity from them, but doesn't accept energy from customers, which means the railway operator cannot get any cash back when the recovered braking energy is fed back to PGC. Therefore, the optimization of TPSS must consider the above policy and pursue the minimum energy cost.

For the TPSS shown in Fig. 1, all substations are connected to two medium voltage buses (MVB) alternatively. If the train braking energy fed back to two buses is equal, the braking energy can be made full use by the loads on the two buses. The maximum benefit of braking energy recover can be enjoyed by railway operator.

Fig. 12 shows the simplified system topology and energy flow diagram of TPSS, where Load1 and Load2 denote all loads on each MVB respectively.

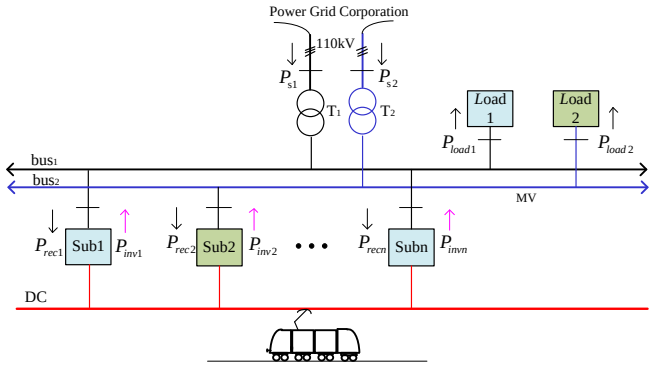

Fig. 12. Simplified system topology and energy flow diagram

The instant power of each MVB can be written as:

$$P_{\text{sup1}}(t) = \sum \left(P_{rec1}(t) + P_{rec3}(t) + \cdots + P_{rec(n-1)}(t)\right) - \sum \left(P_{inv1}(t) + P_{inv3}(t) + \cdots + P_{inv(n-1)}(t)\right) - P_{load1}(t) \quad (10)$$

$$P_{\text{sup2}}(t) = \sum \left(P_{rec2}(t) + P_{rec4}(t) + \cdots + P_{rec(n)}(t)\right) - \sum \left(P_{inv2}(t) + P_{inv4}(t) + \cdots + P_{inv(n)}(t)\right) - P_{load2}(t) \quad (11)$$

where P_{recx} denotes the rectifying power at AC side of each substation, and P_{invx} denotes the inverting power of each substation, x=1,2,…,n.

$$\begin{cases} P_{\text{recx}}(t) = U_{subx}(t) \cdot I_{subx}(t)/\eta_{rec}, when\ I_{subx}(t) > 0 \\ P_{\text{invx}}(t) = U_{subx}(t) \cdot I_{sub1}(t) \cdot \eta_{inv}, when\ I_{subx}(t) < 0 \end{cases} \quad (12)$$

where x=1,2,…n. η_{rec} is the rectifying efficiency and η_{inv} is the inverting efficiency. It is assumed that $\eta_{rec} = 98\%$ and $\eta_{\text{inv}} = 95\%$ in this paper.

The energy consumption of each MVB can be written as:

$$\begin{cases} E_{\text{sup1}} = \int P_{\text{s1}}(t)dt, \ when\ P_{\text{s1}}(t) > 0 \\ E_{\text{inv1}} = \int P_{\text{s1}}(t)dt, \ when\ P_{\text{s1}}(t) < 0 \end{cases} \quad (13)$$

$$\begin{cases} E_{\text{sup2}} = \int P_{\text{s2}}(t)dt, \ when\ P_{\text{s2}}(t) > 0 \\ E_{\text{inv2}} = \int P_{\text{s2}}(t)dt, \ when\ P_{\text{s2}}(t) < 0 \end{cases} \quad (14)$$

$$E_{\text{total}} = E_{\text{sup1}} + E_{\text{sup2}} \quad (15)$$

$$E_{\text{inv}} = E_{\text{inv1}} + E_{\text{inv2}} \quad (16)$$

where $E_{\text{sup1}}$and E_{sup2} are the annual energy consumption from PGC, $E_{\text{inv1}}$and E_{inv2} are the regenerative braking energy fed back to PGC. E_{total} is the total energy consumption per year. E_{inv} is the total energy fed back to PGC.

Assuming the energy price is ρ, the cost of the total energy consumption can be calculated by

$$C_{ele} = \rho \times E_{\text{total}} \quad (17)$$

2) Cost of brake shoes wear, C_{bks}

Train is usually equipped with regenerative braking and friction braking. For energy-saving and brake shoes wear reduction, the regenerative braking is the first choice. However, it can be known from Fig. 6 that the regenerative braking will be reduced or even cancelled when train voltage exceeds U_1, causing significant increase of maintenance cost for brake shoes and metal dust pollution in tunnels.

Friction braking energy can be written as:

$$E_{\text{fric}} = E_{\text{dbk}} - E_{\text{reg}} \quad (18)$$

where E_{dbk} is the demand braking energy per year, E_{reg} is the actual regenerative braking energy per year.

As the wear of brake shoes is directly proportional to the friction braking energy, a price coefficient μ is introduced to calculate the cost of braking shoes wear per year:

$$C_{\text{bks}} = \mu \times E_{\text{fric}} \quad (19)$$

It is worth noting that μ can be obtained from railway operators according to large quantity of maintenance statistics.

3) Cost of inverters per year, C_{inv}

According to [27], the inverter cost consists of the basic component and the component that is linearly dependent on the capacity of inverter (inverter unit price) described in (20).

$$C = C_0 + P_{\text{inv}} \times M_{inv} \quad (20)$$

where P_{inv} is the capacity of the inverter, M_{inv} is the cost per MW.

For a subway line with n traction substations, given the service life of inverter is Y_{life}, the cost of inverters installation per year will be:

$$C_{inv} = C \cdot n/Y_{life} \quad (21)$$

4) Cost objective function, C_{obj}

Given the energy saving, brake shoes wear and economy of inverter, the cost objective function of optimization for inverter operating characteristics can be obtained:

$$C_{obj} = f(P_{max}, r, U_{st}) = C_{ele} + C_{\mathrm{bks}} + C_{inv} \quad (22)$$

Constraints of variables are listed below:

Inverter capacity:

$$P_{max} = 0.5, 1.0, 1.5, 2.0 \text{ MW} \quad (23)$$

where 0.5, 1.0, 1.5 and 2.0 are four possible capacities of the inverters used in the TPSS. In fact, the inverter capacity is not continuous in industrial application.

Start working voltage:

$$U_k \le U_{st} \le U_M \quad (24)$$

where U_k is the no-load voltage of diode rectifier, U_M is the maximum DC voltage. For the real TPSS, U_k is normally 850V, and U_M is normally 950V. U_{st} can be continuously evaluated. For simplicity, it is evaluated with an interval of 10V.

Virtual internal resistance:

$$r_{min} \le \mathrm{r} \le r_{max} \quad (25)$$

where r_{min} and r_{max} are the minimum and maximum virtual internal resistance of the inverter, respectively. It can be seen from Fig. 3 that r_{min} is 0. And r_{max} can be calculated by (2). When $P_{max} = 0.5$ MW, the maximum value of r_{max} is approximately equal to 0.2. It can be seen from section III that $\triangle$r=0.02. For simplicity, r is evaluated with an interval of 0.02.

In addition, it is assumed that the inverter installed in each substation has the same operating characteristic.

IV. OPERATING CHARACTERISTICS OPTIMIZATION CONSIDERING MULTI-TRAINS SCENARIO

Under the actual operation scenario with multi-trains, TPSS turns into a complex time-varying nonlinear system including multiple sources and a lot of moving loads. Therefore, an integrated simulation system is developed to accomplish system energy analysis and parameters optimization.

A. Structure of the integrated simulation system

The integrated simulation system structure considering operating characteristics optimization is shown in Fig. 13. It mainly includes three parts: train motion simulator, system power-flow simulator and cost function calculator. Train motion simulator is developed considering train parameters, route data, speed limits, driving strategies and timetable. Then the electrical power and real-time position of each train can be calculated and used as input data for system power-flow simulation. The system power-flow simulator is formulated from the steady-state model of the traction power supply system. The network admittance matrix can be constructed, then voltage and current of each node in the system can be obtained through iterative calculation [33]. The cost function calculator is specially designed to obtain the value of cost function using the outputs of system power-flow simulator.

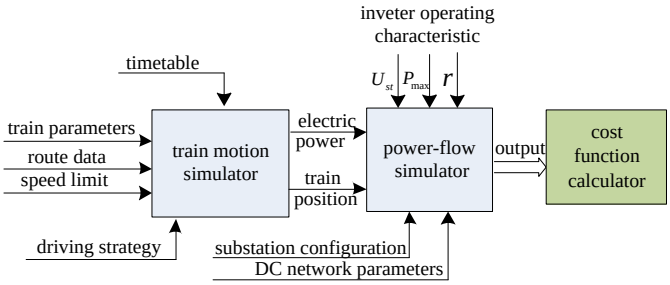

Fig. 13. Integrated simulation system considering operating characteristic optimization for inverter

Fig. 14 shows the simplified network topology of the TPSS. For simplicity, the rail resistance can be included in the overhead contact line [33].

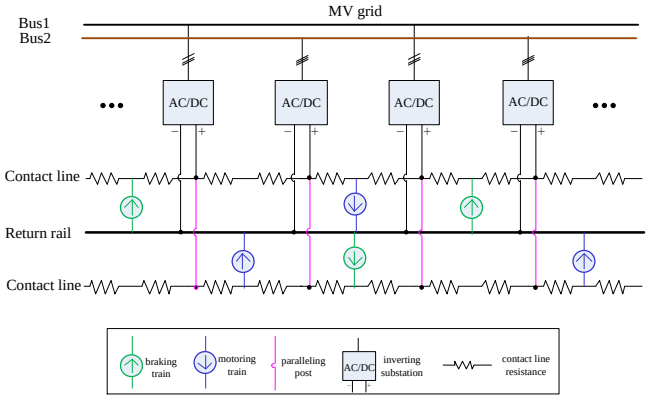

Fig. 14. Simplified network topology of the TPSS

Current injection iterative method is used to solve the power flow [31]. The initial voltage of each train is set to substation no-load voltage according to (26). Thus, the current of each train at next iteration can be calculated and the nodal voltages of the next step are updated in (27). By iterative computation, nodal voltages converge to steady values. The solution then provides the voltage and current for each train on the line.

$$U_{tr\_n}^{(0)} = U_{sub} \quad (26)$$

$$\begin{cases} I_{tr\_n}^{(\mathrm{i}+1)} = \dfrac{P_{tr\_n}}{U_{tr\_n}^{(\mathrm{i})}} \\ \boldsymbol{U}^{(\mathrm{i}+1)} = \boldsymbol{Y}^{-1} \times \boldsymbol{I}^{(\mathrm{i}+1)} \end{cases} \quad (27)$$

where Y^{-1} is the admittance matrix of the power system, U is the voltage vector, I is the current vector.

B. Simulation and calculation parameters

The simulation refers to a typical metro line, which covers a length of 20 km and contains 11 passenger stations and 8 traction substations. All traction substations are inverting substations.

The other simulation parameters are shown in TABLE I.

TABLE I
SIMULATION PARAMETERS IN THE CASE STUDY

Simulation parameters	Value
Headway [s]	600

Terminal turnaround time [s]	300
Contact line resistivity [mΩ/km]	20
Train mass including passengers [ton]	222.8
Motion resistance [kN]	$3.48+0.04025\times v$ $+0.0006575\times v^2$
Maximum operation speed [km/h]	80
Maximum traction power [kW]	3000
Maximum tractive effort [kN]	300
Maximum braking power [kW]	-3000
Maximum braking effort [kN]	-300
AC auxiliary load [kW]	1000

The speed trajectory and power demand of an up-track train are shown in Fig. 15. The following trains will depart after the ahead train by a headway time (600 s), with the same driving profile. When the up-track train arrives at the terminal, it will return back using a down-track driving profile. As the timetable repeats by the headway time, the power flow analysis is computed in a period of 600s in the following simulation.

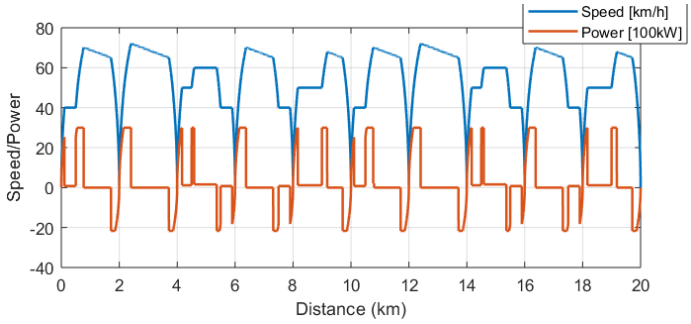

Fig. 15 Driving profile of an up-track train

The other parameters used in the case study are given in TABLE II.

TABLE II
OTHER PARAMETERS IN THE CASE STUDY

Item	Symbol	Value
electricity price for railway	ρ	0.10 USD /kWh
price coefficient for braking shoes wear	μ	0.05 USD /kWh
service life of inverter	Y_{life}	15 years
basic component of inverter cost	C_0	0.15 million USD
capacity related coefficient of inverter	M_{inv}	0.1 USD/W

C. *Impact analysis of inverter operating characteristics*

1) *Impact of r*

When P_{max}=2MW and U_{st}=850V, the demand braking energy and actual regenerative braking energy in the period of 600s can be obtained by simulation, in according to different r. It can be found in Fig. 16 that the regenerative braking energy increases with an decrease in r. When $r < 0.06$, the complete regenerative braking has been realized, which means that the friction braking energy wasted on the braking shoes is zero.

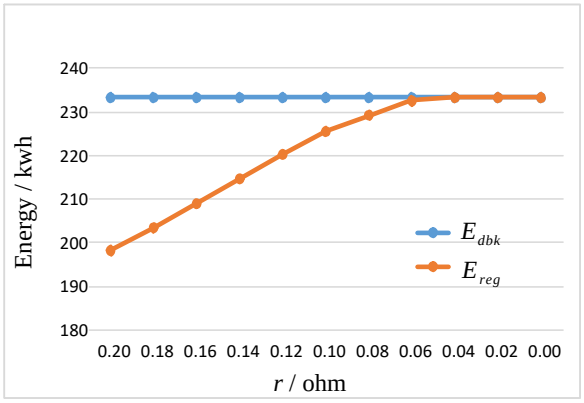

Fig. 16 Demand braking energy and actual regenerative braking energy at different r

It can be seen form Fig. 17 that with the reduction of r, E_{inv1} and E_{inv2} both increase obviously. According to the current energy policy in many countries, the energy fed back to PGC will not bring any benefits to the railway operators.

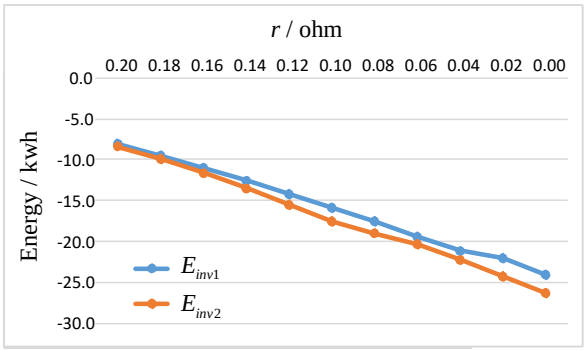

Fig. 17 Energy fed back to the PGC

It can be found from Fig. 18 that with the reduction of r, the total energy consumption E_{total} reduces at first, and then increases. E_{total} reaches the minimal value when r is between 0.6 and 0.8. The reduction of E_{total} at the beginning stage can be attributed to the increase of regenerative braking energy E_{reg}. However, the sharing between two bus bar will get worse due to reduction of r, and the energy fed back the PGC increase faster than the increase of E_{reg}. Therefore, the total energy consumption increase when r becomes smaller than 0.06.

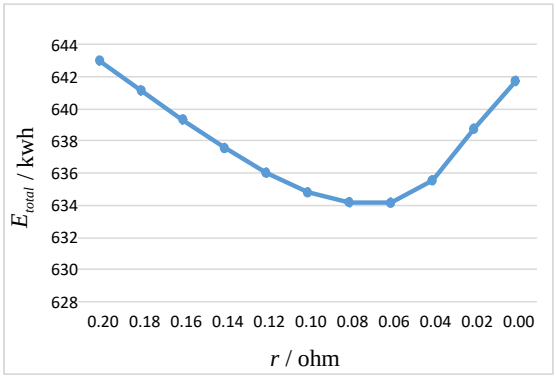

Fig. 18 Total energy consumption changes with *r*

2) Impact of U_{st}

Given that $P_{max} = 1MW$ and $r = 0.06$, the impact of U_{st} is studied. Fig. 19 shows the total energy consumption E_{total} and actual regenerative braking energy E_{reg}. It can be found from that E_{total} increase obviously with the rise of U_{st}. This can be mainly attributed to the fast drop of regenerative braking energy, and lots of braking energy has been exhausted on the braking shoes as heat. Therefore, the U_{st} should be as low as possible, not only for energy saving, but also for braking shoes wear reduction.

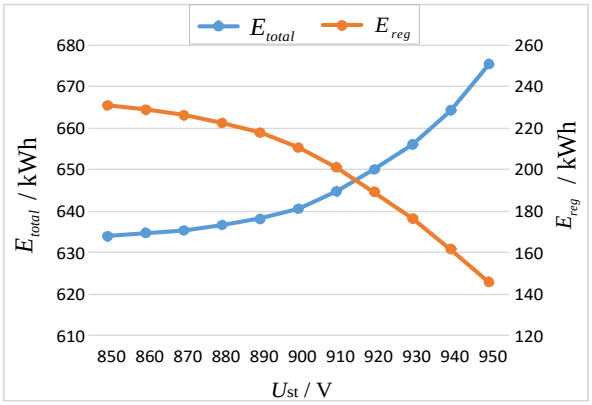

Fig. 19 Total energy consumption changes with U_{st}

3) Impact of P_{max}

Given that $\text{U}_{\text{st}} = 850V$ and $r = 0.06$, the impact of P_{max} is studied. Fig. 20 shows the demand braking energy E_{dbk}, actual regenerative braking energy E_{reg}, and two fed back energy E_{inv1} *and* E_{inv2}. It can be found that E_{dbk} keeps constant and E_{reg} decrease with the reduction of the inverter capacity P_{max}, especially when P_{max} is smaller than 1MW. Meanwhile, the E_{inv1} *and* E_{inv2} both become smaller in magnitude due to the decrease of the E_{reg} of the trains.

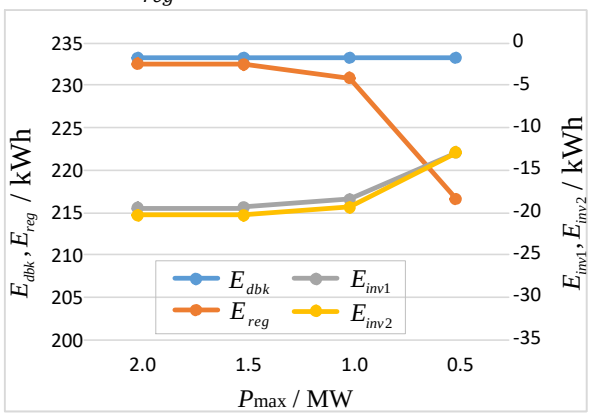

Fig. 20 Typical energy curves at different inverter capacity

Fig. 21 shows the total energy consumption E_{total} and friction braking energy E_{fric} in terms of different inverter capacity P_{max}.

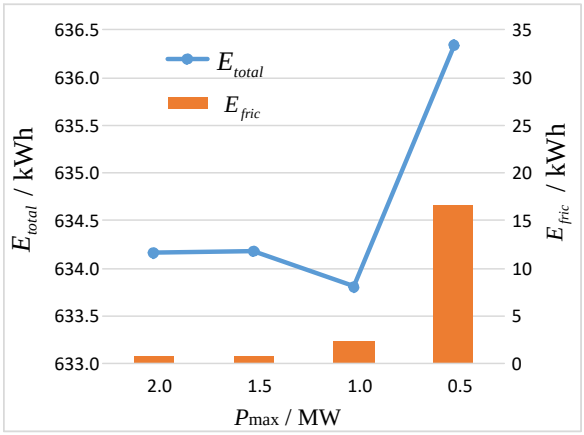

Fig. 21 Total energy consumption and friction braking energy at different inverter capacity

It can be observed from Fig. 21 that E_{fric} increases obviously when P_{max} is smaller than 1.5MW. The change of E_{total} becomes obvious is also when P_{max} is smaller than 1.5MW. However, before that, E_{total} goes through a little decline. Further studies show that the decrease of E_{reg} is smaller than that of E_{inv} when P_{max} change from 1.5MW to 1.0MW. On the contrary, the decrease of E_{reg} is larger than that of E_{inv} when P_{max} change from 1.0MW to 0.5MW, resulting in the increase of E_{total}.

D. Cost function, ObjV

To find the optimal solutions of the cost function, a Brute Force (BF) search algorithm is employed in this paper. It is a straightforward approach to solve problems by enumerating all possibilities in the solution domain.

The BF algorithm used to solve this optimization includes the following steps, which are shown in Fig. 22.

Step1: Confirm the range of control variables, including P_{max} , U_{st} and r. The domain of P_{max} is { 0.5, 1.0, 1.5, 2.0 }. The domain of U_{st} is { 850, 860, 870, 880, 890, 900, 910, 920, 930, 940, 950}. The domain of r is {0, 0.02, 0.04, 0.06, 0.08, 0.10, 0.12, 0.14, 0.16, 0.18, 0.20}.

Step2: Run the integrated simulation system. Calculate cost objective function according to simulation outputs.

Step3: Enumerate all possible solutions in the solution domain. The number of all possible solutions is 484 (=4*11*11).

Step4: Rank the solutions.

Step5: Find the result.

TABLE III shows the cost function results when inverters adopt different operating characteristics. ‘A’ represents that no inverters are installed. ‘B’ represents that 2MW inverters are installed, but no optimization is adopted. ‘C’ represents the proposed optimization method is employed. All costs in the table are calculated in US dollars during one year operation.

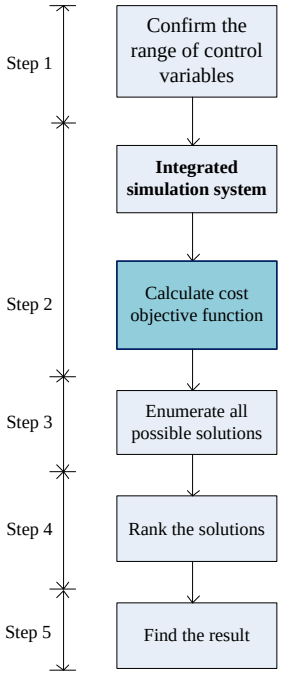

Fig. 22 Flowchart of the Brute Force optimization algorithm

TABLE III
RESULTS COMPARISON

Item	**A** no inverter	**B** not optimized	**C** optimized	**(1-B/A) *100%**	**(1-C/B) *100%**
P_{max}/MW	/	2.0	1.0		
U_{st} /V	/	850	850		
r	/	0.20	0.04		
C_{ele} /M$	3.341	2.840	2.801	15.0%	1.4%
C_{bks} /M$	0.390	0.077	0.003	80.3%	96.1%
C_{inv} /M$	0.000	0.187	0.133	/	28.9%
C_{obj} /M$	3.732	3.104	2.937	16.8%	5.4%

It can be seen from TABLE III that when inverters are not installed, the cost for inverter is zero. The cost for energy consumption is 3.341 M$ per year, and the cost for braking shoes is 0.390 M$ per year. However, when the operating characteristic optimization is not considered, where U_{st}=850V, r=0.20, P_{max}=2MW, the installation of the inverters can reduce the cost for energy consumption by 15%, the cost for braking shoes by 80.3%, and the value of cost function by 16.8%. With the help of the proposed optimization method, the optimal solution is found at P_{max}=1MW, *r*=0.04 and U_{st}=850V. When the optimized results in 'C' are compared with the un-optimized results in 'B', it can be found that the cost of energy consumption is reduced by 1.4% (0.039 M$), the cost for braking shoes is reduced by 96.1% (0.074 M$), the cost of inverter is reduced by 28.9% (0.054 M$), and the value of the cost function is reduced by 5.4% (0.167 M$).

V. CONCLUSION

An optimization method for operating characteristics of inverters used in DC TPSS has been proposed in this paper. The typical application scheme of inverters and its controllable operation characteristics including linear inverting region and constant power region is introduced. A simplified power system model is built to stimulate the impact of power limitation, start working voltage and virtual internal resistance on the amount of regenerative braking energy and its distribution. A cost function considering total energy consumption, brake shoes wear and inverter installation cost is proposed. Based on an integrated simulation system, the BF algorithm is employed to find the optimal operating characteristics of the inverters. The following conclusion can be obtained from this work：

1) The increase of virtual internal resistance of inverter is beneficial to the distribution of regenerative braking energy among substations and better reuse by the AC load of subway, but it will result in higher train voltage and may cause regenerative braking cancellation.
2) The increase of start working voltage will result in the rise of train voltage and the reduction of regenerative braking energy. The friction braking energy on the braking shoes is also increased.
3) Too large inverter capacity will lead to the increase in investment costs, but the effect of energy saving is not obvious. However, too small inverter capacity will lead to significant reduction in regenerative braking energy, and significant increase in brake shoes wear.
4) With the help of the cost function proposed in this paper, the impact of all variables are correlated with cost, so that the multi-objective optimization problem can be transformed into a single objective problem.
5) The results show that, compared with noninverting systems, installing inverters reduce the total costs by 16.8%. By optimizing the operating characteristics of inverters, the total cost is reduced by additional 5.4%.

Note that the headway in the case study is fixed, but in fact, the headway of a subway line is usually different at peak and off-peak time. In our future research, we will pay more attention to the impact of different headway on the final optimal solution.

ACKNOWLEDGMENT

The research work was also supported by the China Scholarship Council.

REFERENCES

[1] A. González-Gil, R. Palacin and P. Batty, "Sustainable urban rail systems: Strategies and technologies for optimal management of regenerative braking energy," Energy Conversion and Management, vol. 75, pp. 374-388, Nov. 2013.

[2] Pieter Hendrik Henning, Heinrich D. Fuchs, Abraham D. le Roux, Hendrik du T. Mouton, "A 1.5-MW Seven-Cell Series-Stacked Converter as an Active Power Filter and Regeneration Converter for a DC Traction Substation", IEEE Transactions on Power Electronics, vol. 23, no. 5, pp. 2230-2236, Sep. 2008.

[3] Y. S. Tzeng, R. N. Wu, N. Chen, "Electric network solutions of DC transit systems with inverting substations", IEEE Trans. Veh. Technol., vol. 47, no. 4, pp. 1405-1412, Nov. 1998.
[4] T. Suzuki, "DC power-supply system with inverting substations for traction systems using regenerative brakes," IEE Proc B Electr Power Appl UK, vol. 129,no. 1, pp. 18-26, Jan. 1982.
[5] B. Mellitt, Z. S. Mouneimne and C. J. Goodman, "Simulation study of DC transit systems with inverting substations," IEE Proceedings B - Electric Power Applications, vol. 131, no. 2, pp. 38-50, Mar. 1984.
[6] N. Ghaviha, J. Campillo, M. Bohlin, and E. Dahlquist, "Review of Application of Energy Storage Devices in Railway Transportation," Energy Procedia, vol. 105, pp. 4561-4568, May, 2017.
[7] T. Ratniyomchai, S. Hillmansen and P. Tricoli, "Recent developments and applications of energy storage devices in electrified railways," IET Electrical Systems in Transportation, vol. 4, no. 1, pp. 9-20, Mar. 2014.
[8] P. Arboleya, B. Mohamed and I. El-Sayed, "DC railway simulation including controllable power electronic and energy storage devices," IEEE Transactions on Power Systems, pp. 1-1, Feb. 2018.
[9] K. Itani, A. De Bernardinis, Z. Khatir, A. Jammal, and M. Oueidat, " Regenerative Braking Modeling, Control, and Simulation of a Hybrid Energy Storage System for an Electric Vehicle in Extreme Conditions," IEEE Transactions on Transportation Electrification. vol. 2, no. 4, pp. 465-479, Dec. 2016.
[10] A. M. Gee and R. W. Dunn, "Analysis of Trackside Flywheel Energy Storage in Light Rail Systems," IEEE Transactions on Vehicular Technology, vol. 64, no.9, pp. 3858-3869, Sep. 2015.
[11] D. Roch-Dupré, Á. J. López-López, R. R. Pecharromán, A. P. Cucala, and A. Fernández-Cardador, "Analysis of the demand charge in DC railway systems and reduction of its economic impact with Energy Storage Systems," International Journal of Electrical Power & Energy Systems, vol. 93, pp. 459-467, Dec. 2017.
[12] S. de la Torre, A. J. Sanchez-Racero, J. A. Aguado, M. Reyes, and O. Martianez, "Optimal Sizing of Energy Storage for Regenerative Braking in Electric Railway Systems," IEEE Transactions on Power Systems, vol. 30, no. 3, pp. 1492-1500, May, 2015.
[13] V. Gelman, "Energy Storage That May Be Too Good to Be True: Comparison Between Wayside Storage and Reversible Thyristor Controlled Rectifiers for Heavy Rail," IEEE Vehicular Technology Magazine, vol. 8, no. 4, pp. 70-80, Dec. 2013.
[14] V. Gelman, "Braking energy recuperation," IEEE Vehicular Technology Magazine, vol. 4, no. 3, pp. 82-89, Sep. 2009.
[15] D. Cornic, "Efficient recovery of braking energy through a reversible dc substation," Proc. ESARS, pp. 1-9, Oct. 2010.
[16] H. Douglas, C. Roberts, S. Hillmansen, and F. Schmid, "An assessment of available measures to reduce traction energy use in railway networks," Energy Conversion and Management, vol. 106, pp. 1149-1165, Dec. 2015.
[17] H. Ibaiondo and A. Romo, "Kinetic energy recovery on railway systems with feedback to the grid," in Proceedings of 14th International Power Electronics and Motion Control Conference EPE-PEMC 2010, Sep. 2010, DOI: 10.1109/EPEPEMC.2010.5606545
[18] J. Nomura, A. Kataoka and K. Inagaki, "Development of a Hybrid Inverter and a Hybrid Converter for an electric railway," 2007 Power Conversion Conference - Nagoya, pp. 1164-1169, Apr. 2007. DOI: 10.1109/PCCON.2007.373112
[19] G. Zhang, Z. Tian, H. Du, and Z. Liu, "A Novel Hybrid DC Traction Power Supply System Integrating PV and Reversible Converters," Energies, vol. 11, no. 7, p. 1661, Jun. 2018.
[20] G. Zhang, J. Qian and X. Zhang, "Application of a High-Power Reversible Converter in a Hybrid Traction Power Supply System," Applied Sciences, vol. 7, no. 3, p. 282, Mar. 2017.
[21] M. Popescu, A. Bitoleanu, V. Suru, and A. Preda, "System for converting the DC traction substations into active substations," The 9th International Symposium on Advanced Topics in Electrical Engineering (ATEE), pp. 632-637, May. 2015. DOI: 10.1109/ATEE.2015.7133893
[22] C. V. Suru, M. Popescu and A. Bitoleanu, "Control algorithm implementation for a filtering and regeneration system used in urban traction DC substations," 2016 International Symposium on Power Electronics, Electrical Drives, Automation and Motion (SPEEDAM), Jun. 2016, pp. 651-656.
[23] A. Bitoleanu, M. Popescu and C. V. Suru, "Theoretical and experimental evaluation of the indirect current control in active filtering and regeneration systems," 2017 International Conference on Optimization of Electrical and Electronic Equipment (OPTIM) & 2017 Intl Aegean Conference on Electrical Machines and Power Electronics (ACEMP), May. 2017, pp. 759-764. DOI: 10.1109/OPTIM.2017.7975060
[24] M. Popescu, A. Bitoleanu and M. Dobriceanu, "FBD-based control in active DC-traction substations," in 2016 International Conference on Applied and Theoretical Electricity (ICATE), 2016, pp. 1-6.
[25] R. Liu, W. Liu, H. Cui, J. Zhang, and J. Liao, "Capacity optimization design of reactive compensation device in urban rail traction power supply system," in 2017 IEEE Transportation Electrification Conference and Expo, Asia-Pacific (ITEC Asia-Pacific), 2017, pp. 1-6.
[26] Z. Zhu, "Research on Reactive Power Compensation Scheme and Compensation Capacity of Subway Power Supply System," The World of Inverters, vol. 11, pp. 45-47, 2014.
[27] W. Jefimowski and A. Szeląg, "The multi-criteria optimization method for implementation of a regenerative inverter in a 3 kV DC traction system," Electric Power Systems Research, vol. 161, pp. 61-73, Aug. 2018.
[28] C. H. Bae, "A simulation study of installation locations and capacity of regenerative absorption inverters in DC 1500V electric railways system," Simulation Modelling Practice and Theory, vol. 17, no. 5, pp. 829-838, May. 2009.
[29] C. H. Bae, M. S. Han, Y. K. Kim, C. Y. Choi, and S. J. Jang, "Simulation Study of Regenerative Inverter for DC Traction Substation," in 2005 International Conference on Electrical Machines and Systems, 2005, pp. 1452-1456. DOI: 10.1109/ICEMS.2005.202789
[30] P. Arboleya, "Heterogeneous Multiscale Method for Multirate Railway Traction Systems Analysis," IEEE Transactions on Intelligent Transportation Systems, vol. 18, no. 9, pp. 2575-2580, Sep. 2017.
[31] B. Wang, Z. Yang, F. Lin, and W. Zhao, "An Improved Genetic Algorithm for Optimal Stationary Energy Storage System Locating and Sizing," Energies, vol. 7, no. 10, pp. 6434-6458, Oct. 2014.
[32] M. Soler, J. Lopez, J. M. Mera Sanchez De Pedro, and J. Maroto, "Methodology for Multiobjective Optimization of the AC Railway Power Supply System," IEEE Transactions on Intelligent Transportation Systems, vol. 16, no. 5, pp. 2531-2542, Oct. 2015.
[33] Z. Tian, P. Weston, N. Zhao, S. Hillmansen, C. Roberts, and L. Chen, "System energy optimisation strategies for metros with regeneration," Transportation Research Part C Emerging Technologies, vol. 75, pp. 120-135, Feb. 2017.

Gang Zhang was born in Chongqing, China. He received his B.Eng. and Ph.D. degree in School of Electrical Engineering from Beijing Jiaotong University, Beijing, China, in 2005 and 2010, respectively. From 2010 to 2012, he worked as a post-doctor at Tsinghua university, where he was engaged in research on high power grid-connected power converter. He is currently a Lecture in the School of Electrical Engineering, Beijing Jiaotong University, Beijing, China. His current research interests focus on power electronics and control, which includes high power traction power converter, grid-connected inverter, and energy-saving techniques in subway.

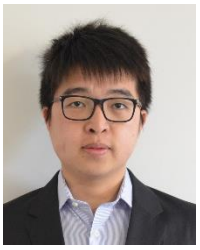

Zhongbei Tian received the B.Eng in Huazhong University of Science and Technology, Wuhan, China, in 2013. He received the B.Eng. and PhD degree in Electrical and Electronic Engineering from the University of Birmingham, Birmingham, U.K., in 2013 and 2017. He is currently a Research Fellow at the University of Birmingham. His research interests include railway traction system and power network modeling, energy systems optimization, advanced traction power systems design, analysis of electric railways.

Pietro Tricoli (M'06) received the M.S. (cum laude) and Ph.D. degrees in Electrical Engineering from the University of Naples Federico II, Italy, in 2002 and 2005, respectively. He is currently a Senior Lecturer of Electrical Power and Control in the Department of Electronic, Electrical, and Systems Engineering, University of Birmingham, Birmingham, U.K. His research focusses on modeling and control of power converters with application to storage devices for electric vehicles, railway electrification and traction systems, wind and photovoltaic generation.

Stuart Hillmansen received his Ph.D. degree from Imperial College, London. He is currently a Senior Lecturer in electrical energy systems with the Department of Electronic, Electrical, and Systems Engineering at the University of Birmingham. He is a member of the Birmingham Centre for Railway Research and Education where he leads the Railway Traction Research Group, whose portfolio of activities is supported by the railway industry and government. His research interests include hybrid traction systems for use in railway vehicles and the modeling and measurement of energy consumption for railway systems.

Yong Wang was born in Liaocheng, China. He received his B.Eng. degree in School of Electrical Engineering from Shandong University of Science and Technology, Shandong, China, in 2011,and obtained his master's degree in School of Electrical Engineering from Beijing Jiaotong University, Beijing, China, in 2017. He works since 2017 in Institute of standards and metrology China academy of railway sciences group co., LTD, where he engage in research on standard of railway product, product testing and supervision and spot checks, His main research interests include high-power power electronic devices, energy-saving techniques in subway, the subway and EMU traction auxiliary inverter, and EMU electronic device .

Zhigang Liu was born in Shandong, China. He received his B.Eng. and Ph.D. degree in School of Electrical Engineering from Beijing Jiaotong University, Beijing, China, in 1986 and 1994, respectively. He is currently a professor in the School of Electrical Engineering, Beijing Jiaotong University, Beijing, China. His current research interests include AC drives, traction power supply system, power electronic circuit and system, computer network communication, and industrial automation technology.